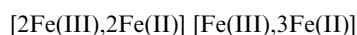
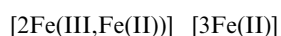
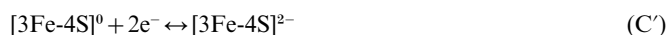


electrodes [13]. Protein film voltammetry affords a rapid and precise way to induce and monitor interconversion of 4Fe and 3Fe clusters, because the protein molecules under investigation are confined to the electrode surface and are therefore under tight potential control, and the presence of a [3Fe-4S] cluster can be ascertained immediately from the appearance of a characteristic pair of signals (corresponding oxidation and reduction peaks) in the cyclic voltammogram (CV) [18–20]. The first of these (termed A'; see below) arises from the well-known one-electron [3Fe-4S]⁺⁰ couple, whereas the second (C') at more negative potential is assigned to the two-electron [3Fe-4S]^{0/2-} couple – an unusual, co-operative two-electron transfer that produces sharp and diagnostically useful peaks [21,22]:



The 'A'C' pair signifies the presence of a [3Fe-4S] cluster. Referenced against the signal (B') due to the [4Fe-4S] cluster, the relative populations of [4Fe-4S] and [3Fe-4S] clusters in the sample at any time following a pulse is easily monitored, since peak areas are proportional to the number of electrons transferred at each site.

In the present study, we have applied protein film voltammetry with oxidative pulses to examine and quantify the process of oxidative degradation of [4Fe-4S] clusters in several ferredoxins, most of which have been well characterized spectroscopically. These include reconstituted 8Fe *Azotobacter vinelandii* FdI (*AvFdI*) and three mutant variants [$\Delta\text{Thr}^{14}/\Delta\text{Asp}^{15}$, $\text{Thr}^{14} \rightarrow \text{Cys}$ (T14C) and C42D], all of which are known to have a cluster that can exist in both [3Fe-4S] and [4Fe-4S] forms [23–26]. The electrochemical data have been correlated with air-sensitivities of these proteins, and we have explored the likelihood of wider applicability by examining other ferredoxins. One of these (*DaFdIII*) contains a [3Fe-4S] and a [4Fe-4S] cluster, two [*Pyrococcus furiosus* Fd (*PfFd*) and *CpFd*] contain, respectively, one and two air-stable [4Fe-4S] clusters, and one [*Thauera aromatica* Fd (*TaFd*)] contains two air-sensitive [4Fe-4S] clusters [27–30]. The results show that for these proteins (and unlike HiPIPs) the stability of the [4Fe-4S] clusters towards degradation under ambient aerobic conditions is largely determined by the reduction potential of oxidative processes that produce labile hypervalent states (initially [4Fe-4S]³⁺).

EXPERIMENTAL

Purified water (Millipore; resistivity $\approx 18 \text{ M}\Omega \text{ cm}$) was used in all experiments. The buffers Mes, Hepes and Taps, and co-adsorbate polymyxin B sulphate, were purchased from Sigma, whereas other reagents were obtained from Aldrich or BDH and were of at least analytical grade. All voltammetry experiments were performed anaerobically in a glove box (Vacuum Atmosphere Company, Hawthorne, CA, U.S.A.; or Belle Technology, Poole, Dorset, U.K.) with an inert atmosphere of N_2 ($\text{O}_2 < 2.0 \text{ p.p.m.}$).

Native *AvFdI* was purified as described before [31]. Preparation of the 8Fe form was performed as described previously, except

that 15% (w/v) trichloroacetic acid was used for cluster removal [23]. The final product had an absorbance ratio A_{390}/A_{280} of 0.56. The mutants $\Delta\text{Thr}^{14}/\Delta\text{Asp}^{15}$, T14C and C42D were obtained in earlier procedures, as were samples of *TaFd* and *DaFdIII* [24–27,30]. Cells of *P. furiosus* were supplied by the Centre for Applied Microbiology and Research, Porton Down, Salisbury, Wilts., U.K., and samples of *PfFd* in either 3Fe or 4Fe forms were prepared by procedures published previously [4,28].

An AutoLab electrochemical analyser (EcoChemie, Utrecht, The Netherlands) equipped with GPES software and a low-current detection module was used in conjunction with an all-glass cell and three-electrode system [32]. Before each experiment, the pyrolytic graphite 'edge' electrode (surface area 0.18 cm^2) was polished with an aqueous slurry of alumina (Buehler Micro-polish; $1.0 \mu\text{m}$) and sonicated extensively. All potentials are given with reference to the standard hydrogen electrode ('SHE'). The saturated calomel reference electrode ('SCE') was held at 22°C , at which we have adopted $E(\text{SCE}) = +243 \text{ mV}$ as measured against the SHE, while the sample compartment was maintained at 0°C .

Before voltammetry, the protein samples were pre-purified anaerobically by FPLC (Mono Q column; Pharmacia). Solutions were then dialysed into the required buffer solutions using an Amicon 8MC unit equipped with a microvolume assembly and a YM3 membrane. The ferredoxin solution (typically 0.1 mM) used to coat the electrode typically contained 0.1 M NaCl and a 60 mM mixed-buffer system (15 mM each of acetate, Mes, Hepes and Taps), with $200 \mu\text{g/ml}$ polymyxin to stabilize the film [31,32]. Unless otherwise stated, $400 \mu\text{l}$ of this solution was also placed in the electrochemical cell. To produce protein films, the freshly polished electrode surface was painted with $\approx 1 \mu\text{l}$ of chilled protein solution from a fine capillary, then placed promptly into the cell. For analysis, CVs were corrected for non-Faradaic background current by subtracting a polynomial baseline, assuming that all the electrochemical activity lies under the compact peaks [33]. Reduction potentials (E^0) were calculated from the average of the oxidation and reduction peak potentials.

Pulsing experiments were performed as described previously [13]. The protein-coated electrode was cycled, typically at $50 \text{ mV}\cdot\text{s}^{-1}$, over the normal potential range until the voltammetry had stabilized (usually three scans). This procedure yields a film of protein molecules at a coverage consistent with an electroactive monolayer. The protein film was then subjected to an oxidative pulse at various potentials, between 0.4 and 0.7 V , for 1 – 20 s . A CV was scanned immediately afterwards in the normal potential region to observe the changes that had occurred.

For native *AvFdI*, excursions (rather than pulses) to oxidizing potentials were also used. This involved running CVs from the normal low-potential region up to the high potentials that trigger cluster degradation. As the scan returns from the high-potential region, the changes that have occurred are revealed in the CV.

In the report that follows, the 'normal region' for reversible redox couples of the Fe/S clusters will be emphasized by inclusion of a negative sign (e.g. as in -400 mV), whereas oxidative processes will be signified by inclusion of a '+' sign.

RESULTS

To aid discussion, the amino-acid sequences of the different proteins that have been studied are shown in Figure 1.

Native *AvFdI*

Native *AvFdI* is normally a 7Fe protein that contains one [4Fe-4S]^{2+/+} and one [3Fe-4S]⁺⁰ cluster; however, when reconstituted

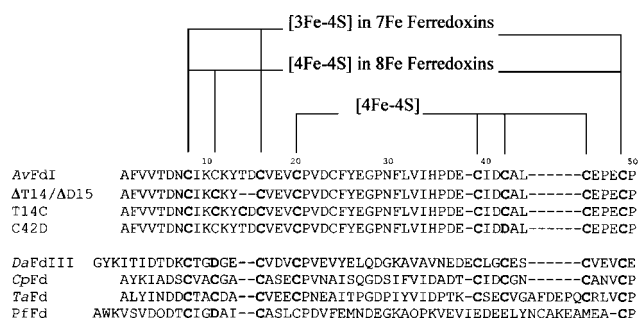


Figure 1 Comparisons among the amino acid sequences of the ferredoxins examined in this study

These are numbered according to the sequence of *AvFdl*.

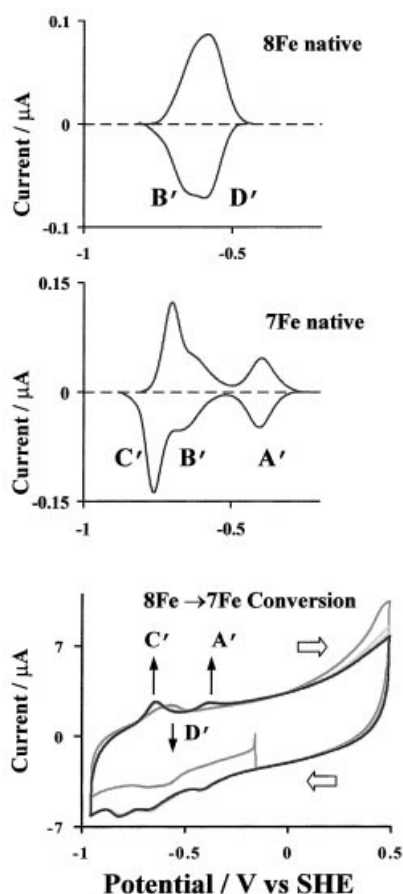


Figure 2 Baseline-subtracted film voltammograms of the reconstituted 8Fe form (top panel) and the 7Fe native form (middle panel) of *AvFdl* at 20 mV s^{-1} , pH 7.4 and 0°C , and the conversion of 8Fe *AvFdl* into the 7Fe form induced by sweeping to $+493 \text{ mV}$ at 75 mV s^{-1} , pH 7.4 and 0°C (bottom panel)

SHE, standard hydrogen electrode.

from apoprotein, using inorganic iron and sulphide, it refolds as an 8Fe protein [23]. Figure 2 shows the baseline-subtracted film voltammograms of the 8Fe form of *AvFdl* (top panel) and the native 7Fe form (middle panel), each measured at pH 7.4 and

0°C . The 8Fe form produces a single, broad asymmetric peak in both reductive and oxidative directions, which arises from the overlapping signals (termed B' and D'; the 'prime' signifying that the protein is immobilized on the electrode and is not free in solution) of the two $[4\text{Fe-4S}]^{2+/+}$ clusters; deconvolution of the envelope yields reduction potentials of -615 mV and -555 mV respectively. As discussed below, the more negative component (B') is assigned to the $[4\text{Fe-4S}]^{2+/+}$ cluster that is indigenous in the 7Fe form, whereas D' at -555 mV stems from the 'new' $[4\text{Fe-4S}]$ cluster that is introduced in the 8Fe form.

The bottom panel of Figure 2 shows the transformation of 8Fe to 7Fe *AvFdl* that occurs rapidly when a film of the 8Fe form is scanned to the oxidizing potential of $+493 \text{ mV}$ at a rate of 75 mV s^{-1} . Two new signals are clearly seen: signal A' (at -420 mV) and signal C' (average peak value -756 mV) correspond to the $[3\text{Fe-4S}]^{0/+}$ and the $[3\text{Fe-4S}]^{0/2-}$ transitions respectively in the native 7Fe ferredoxin. As these new signals appear, the broad signal due to the two $[4\text{Fe-4S}]$ clusters diminishes, with the higher-potential component (D') vanishing: this observation corresponds to conversion of this $[4\text{Fe-4S}]$ cluster into $[3\text{Fe-4S}]$. Contrary to what is observed with other proteins, short pulses at $+493 \text{ mV}$ gave complete and selective degradation of the higher-potential $[4\text{Fe-4S}]$ cluster, with no noticeable formation of $[3\text{Fe-4S}]$. No other signals were observed, either after oxidative scanning or pulsing; e.g. as might correspond to a $[4\text{Fe-3S}]$ species produced when native 7Fe *AvFdl* is reacted with $\text{Fe}(\text{CN})_6^{3-}$ [34].

$\Delta\text{Thr}^{14}/\Delta\text{Asp}^{15}$ *AvFdl*

In the double mutant $\Delta\text{Thr}^{14}/\Delta\text{Asp}^{15}$, deletion of two residues introduces the classical $[4\text{Fe-4S}]$ cluster-binding motif into the region of the $[3\text{Fe-4S}]$ cluster (see Figure 1), resulting in an 8Fe protein that degrades to a 7Fe protein upon exposure to oxygen [24]. Figure 3 shows the baseline-subtracted voltammetry of different states of $\Delta\text{Thr}^{14}/\Delta\text{Asp}^{15}$ *AvFdl*.

The 8Fe form (top panel) displays two signals due to reversible couples, which are clearly seen at -466 mV and -642 mV at pH 7.0. We assign the lower-potential signal to the unaltered $[4\text{Fe-4S}]$ cluster, and it is therefore labelled B', as in the 7Fe protein. Signal D' (which is sharper, but still consistent with a one-electron reaction) is assigned to the 'new' $[4\text{Fe-4S}]$ cluster. After pulsing a film at $+543 \text{ mV}$ for 4 s, new signals A' and C', typical of a $[3\text{Fe-4S}]$ cluster, appear at -147 mV and -757 mV (Figure 3, middle panel). This transformation occurs with the simultaneous decrease in the signal (D') due to the higher-potential $[4\text{Fe-4S}]$ cluster at -466 mV , consistent with its conversion into a $[3\text{Fe-4S}]$ cluster. After the pulse, the 'new' $[4\text{Fe-4S}]$ cluster is not completely converted, as some of the -466 mV signal remains. In a previous report [24], it was concluded that the $[3\text{Fe-4S}]^{0/+}$ product of this transformation has a reduction potential very similar to the parent $[4\text{Fe-4S}]^{2+/+}$ cluster: it is now evident that its reduction potential, at -147 mV , is over 300 mV more positive than that of the $[4\text{Fe-4S}]^{2+/+}$ cluster. This difference is consistent with observations made for other interconverting 3Fe/4Fe systems, where the $[3\text{Fe-4S}]^{0/+}$ cluster is noted to have a significantly higher potential than its $[4\text{Fe-4S}]^{2+/+}$ counterpart [4,5,20,35]. In our previous study, signal A' was not clearly observed, because the sample that was analysed contained mainly 8Fe protein with only small amounts of 7Fe protein.

Metal-ion uptake into $[3\text{Fe-4S}]$ clusters has been studied in several proteins, and this was now investigated in $\Delta\text{Thr}^{14}/\Delta\text{Asp}^{15}$ *AvFdl*. When the 8Fe protein is pulsed with 25 mM Fe^{2+} in solution, the $[3\text{Fe-4S}]$ cluster that is formed reverts slowly back

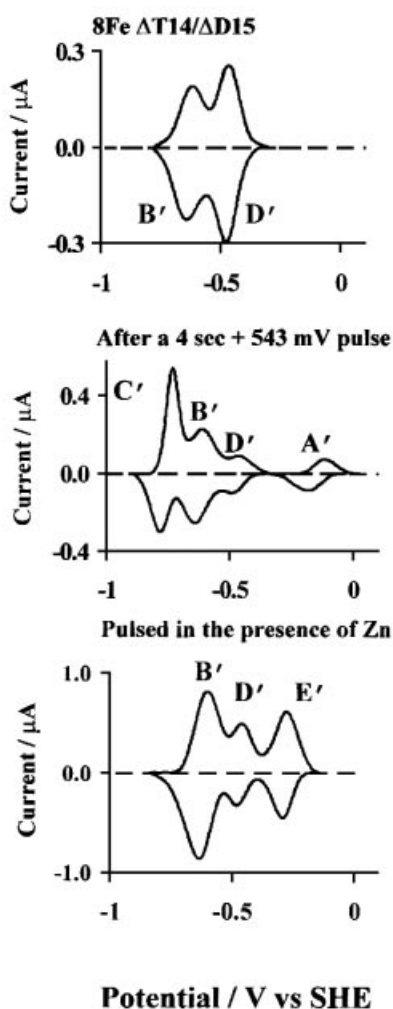


Figure 3 Background-subtracted film voltammograms of the 7Fe and 8Fe forms of $\Delta\text{Thr}^{14}/\Delta\text{Asp}^{15}$ AvFdl recorded at $50 \text{ mV} \cdot \text{s}^{-1}$, pH 7.0 and 0°C

Top panel: the 8Fe form as prepared. Middle panel: the voltammetry after a 4 s pulse at +543 mV, which generates a high proportion of the 7Fe form. Bottom panel: the voltammogram of the product obtained by pulsing a film of 8Fe protein at +543 mV for 4 s in the presence of 5 mM Zn^{2+} . SHE, standard hydrogen electrode.

to [4Fe-4S], re-establishing the 8Fe form. When pulsed in the presence of 5 mM Zn^{2+} , the [3Fe-4S] cluster that is formed reacts rapidly to produce a Zn adduct (tentatively assigned as $[\text{Zn}3\text{Fe-4S}]^{2+/+}$ on the basis of previous studies) [4,5,13,20,35,36], characterized by a signal with a reduction potential of -286 mV (labelled E' in Figure 3, bottom panel). As with pulsing experiments without Zn^{2+} present, not all [4Fe-4S] clusters are converted into Zn products during the pulse, and some unaltered signal D' remains.

The pH-dependence of the reduction potential for the [3Fe-4S] $^{+/0}$ couple in native AvFdl shows that a single proton is taken up with a $\text{p}K_a$ of 7.8 [31,37]. In contrast, the reduction potential of the [3Fe-4S] $^{+/0}$ couple in $\Delta\text{Thr}^{14}/\Delta\text{Asp}^{15}$ AvFdl shows little pH-dependence (results not shown), similar to the [3Fe-4S] cluster in DaFdlIII [27]. Figure 4 shows the levels of [3Fe-4S] cluster formed from 8Fe $\Delta\text{Thr}^{14}/\Delta\text{Asp}^{15}$ AvFdl when the protein film is pulsed for 4 s at different oxidative potentials. The

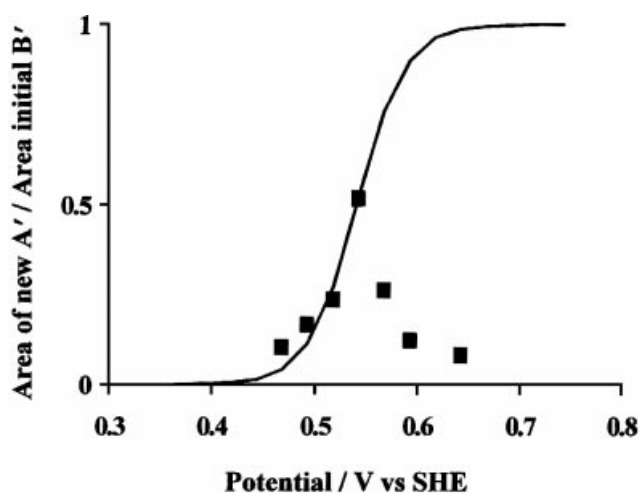


Figure 4 Plot of the amount of [3Fe-4S] cluster present in $\Delta\text{Thr}^{14}/\Delta\text{Asp}^{15}$ AvFdl, after a 4 s pulse at various potentials, pH 7.0, 0°C

A 'best-fit' Nernstian sigmoid (transition potential; +540 mV) is also shown. SHE, standard hydrogen electrode.

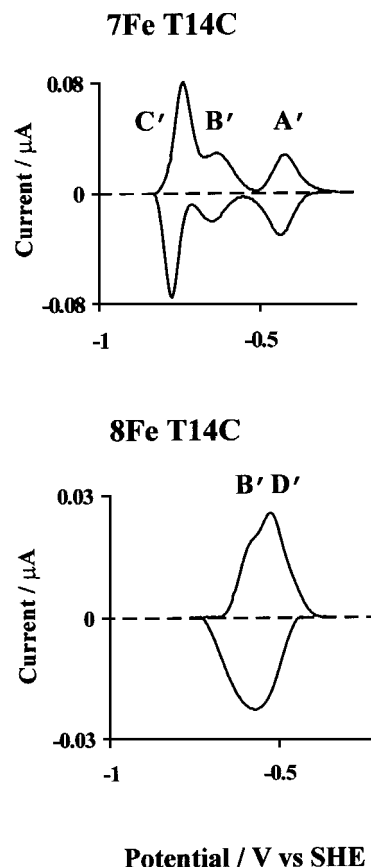


Figure 5 Background-subtracted film voltammograms of the 7Fe and 8Fe forms of T14C AvFdl, recorded at $10 \text{ mV} \cdot \text{s}^{-1}$, pH 8.0 and 0°C

SHE, standard hydrogen electrode.

sigmoidal line is the best attempt to fit the data to an effective 'transformation' potential for the rising part of the data, and in this case a one-electron fit gives a value of +540 mV.

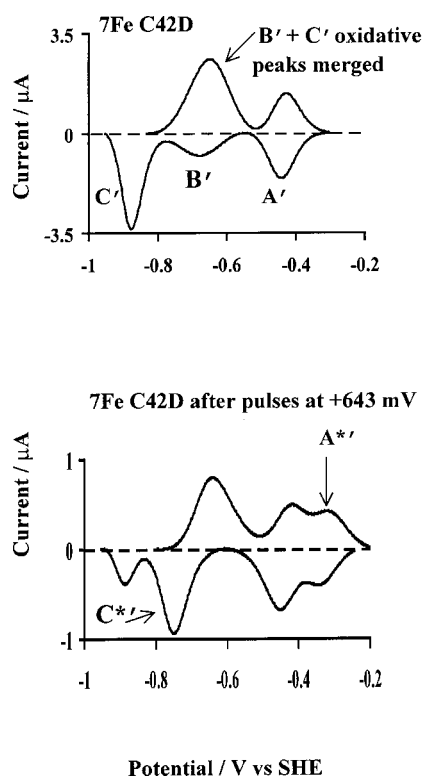


Figure 6 Background-subtracted film voltammograms of C42D AvFdl recorded at 50 mV·s⁻¹, pH 8.0 and 0 °C

Upper panel: the 7Fe form; lower panel: the product obtained after a sequence of +643 mV pulses for 4, 3 and then 2 s. A second [3Fe-4S] cluster is formed, as evidenced by the new features A* and C*. SHE, standard hydrogen electrode.

T14C AvFdl

The mutant T14C AvFdl introduces an additional cysteine (C*) residue into the [3Fe-4S] cluster region of the protein in an attempt to create a classic motif CxxCxxC* (Figure 1), where 'x' denotes 'any amino acid residue' [25]. When the cells are opened and the protein is purified in the presence of dithionite, an 8Fe protein is recovered, whereas without dithionite a 7Fe form is produced. As with native AvFdl, the 7Fe protein clearly shows three signals (Figure 5, upper panel): these are the A', B' and C' couples, with reduction potentials of -426, -633 and -756 mV respectively at pH 8.0. Figure 5 (lower panel) shows the baseline-subtracted voltammetry of the 8Fe form: the reduction potentials of the [4Fe-4S]^{2+/+} clusters are approx. -519 mV and -565 mV (measured by square wave voltammetry), although it is unclear which signal belongs to the indigenous [4Fe-4S] cluster. The change in potential of the indigenous [4Fe-4S] cluster relative to that in the 7Fe form is possibly due to alterations in the protein backbone around the cluster.

Pulsing or sweeping to a potential of +568 mV did not produce any notable amounts of [3Fe-4S] cluster, even when performed in the presence of 2 mM EGTA, while accessing potentials above +568 mV resulted only in a general signal loss.

C42D AvFdl

To probe how aspartate ligation of one subsite might destabilize a [4Fe-4S] cluster, a C42D variant of AvFdl was produced [26]. This introduces an aspartate ligand into the site of the central

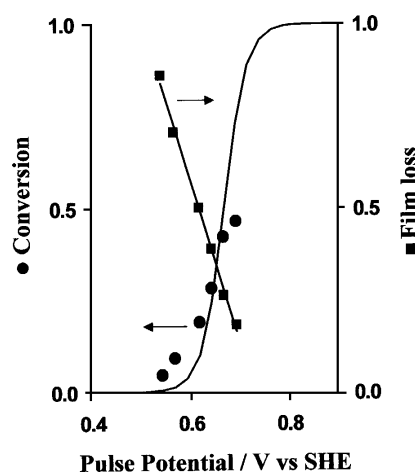


Figure 7 Plot showing the amount of [3Fe-4S] cluster present in a film of C42D AvFdl, after a 4 s pulse, as a function of the pulsing potential, at pH 8.0, 0 °C

A 'best fit' Nernstian sigmoid, transition potential +670 mV, has been added. The right-hand axis shows protein film loss, followed by measuring the area of the A' couple signal after a pulse. SHE, standard hydrogen electrode.

cysteine co-ordinating the [4Fe-4S] cluster (this occupies a typical [4Fe-4S] cluster-binding domain) thus creating a CxxDxxC sequence similar to those of PfFd and DaFdIII, proteins for which interconversion between [3Fe-4S] and [4Fe-4S] forms has been well documented [6,38]. In DaFdIII, the Fe atom occupying the aspartate position is only weakly co-ordinated: the dissociation constant K_d for [4Fe-4S]²⁺ is 30 μM, and metals such as Zn or Cd are bound more tightly [6]. Aspartate ligation has not been confirmed in DaFdIII, but is established by NMR for PfFd and by crystallography for C42D AvFdl [26,39].

When C42D was purified, it was found that it produces an air-stable 7Fe protein just like the native form, and attempts by chemical means to convert the [4Fe-4S] cluster into a second [3Fe-4S] cluster were unsuccessful [26]. However, the electrochemical pulsing technique proved to be successful, and Figure 6 shows the conversion of 7Fe C42D AvFdl into the 6Fe form at pH 8.0. The 7Fe film data (Figure 6, upper panel) shows reduction peaks from each of the A', B' and C' signals, corresponding to the [3Fe-4S]⁺⁰, [4Fe-4S]^{2+/+} and [3Fe-4S]^{0/2-} redox couples respectively, noting that, as a consequence of the large peak separation of the [3Fe-4S]^{0/2-} couple at 50 mVs⁻¹, the C' and B' oxidative peaks overlap. To convert the 7Fe protein into the 6Fe form, the film was pulsed at a potential of +643 mV for 4 s, 3 s and finally 2 s, with voltammograms recorded between pulses. After this pulse sequence, new signals indicative of the formation of a second [3Fe-4S] cluster were obtained (Figure 6, lower panel). Signal B' from the indigenous [4Fe-4S] cluster has disappeared and two signals, labelled A* and C* (* is used to distinguish them from the indigenous [3Fe-4S] cluster couples), have appeared at -334 mV and -760 mV (reductive peak position for C*). These signals are assigned to the new [3Fe-4S] cluster. As noted previously, signal C' from the indigenous [3Fe-4S] cluster is diminished in size after pulsing, and no longer displays a 2:1 ratio with the A' couple. This also occurs upon pulsing the native protein, and the reason for this behaviour remains unclear [26]. From its pH-dependence, the new A* couple shows a pK_a of 7.7, similar to the [3Fe-4S] cluster in the

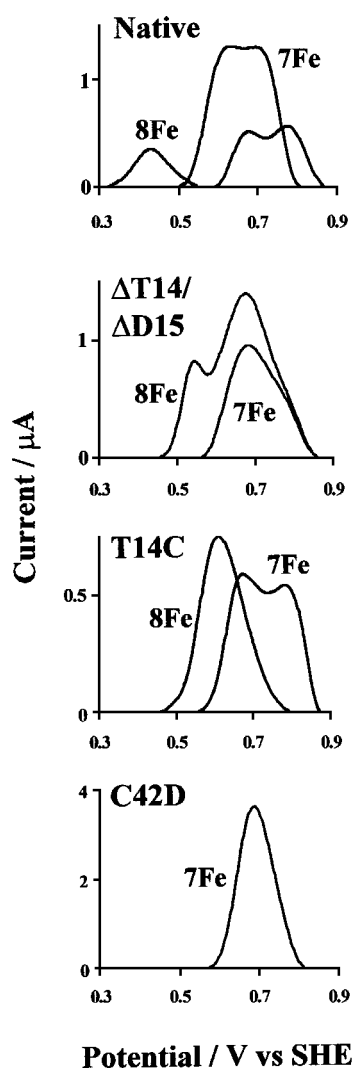


Figure 8 High-potential voltammograms (background-subtracted, oxidation direction only) recorded for native, $\Delta\text{Thr}^{14}/\Delta\text{Asp}^{15}$, T14C and C42D forms of *AvFdI* at pH 7.0, 0 °C

SHE, standard hydrogen electrode.

native protein (pK_a 7.8) [26,31]. Films of the 6Fe form of the protein were transferred to 5 mM solutions of Zn^{2+} and Fe^{2+} , but unlike $\Delta\text{Thr}^{14}/\Delta\text{Asp}^{15}$ *AvFdI*, no evidence of metal uptake was observed.

As with $\Delta\text{Thr}^{14}/\Delta\text{Asp}^{15}$ *AvFdI*, the levels of [3Fe-4S] cluster formed during a 4 s pulse, at varying pulsing potentials, were examined (Figure 7, left axis). This was performed by estimating the peak area attributable to the new signal A^* after a pulse (normalized with respect to total film loss by dividing by the area attributable to the indigenous A' signal); the data are shown alongside their best fit to a Nernstian sigmoid, with a transition potential of +670 mV. The fit is not good and it is largely due to the difficulty in measuring the peak areas at higher potentials: peak areas observed following pulses above +700 mV were not recorded, since signal loss was too great for the areas to be measured accurately. The total amount of signal loss after a pulse is shown in Figure 7 (right axis); this was obtained by

measuring the loss of signal A' peak area after pulsing, with a pulse at +643 mV for 4 s resulting in approx. 75% loss.

High-potential voltammetry for variants of *AvFdI*

To probe the oxidative processes leading to degradation of [4Fe-4S] clusters and the formation of [3Fe-4S] clusters, CV between 300 and 900 mV was performed on all proteins. Figure 8 shows the oxidative peaks (after background subtraction) that were observed for the 7Fe forms and, where applicable, the 8Fe forms of the variants of *AvFdI*.

In the 8Fe forms of native and $\Delta\text{Thr}^{14}/\Delta\text{Asp}^{15}$ *AvFdI* (where one of the two [4Fe-4S] clusters is more susceptible to oxidative degradation than the other), it is important to be able to compare the signals produced by the 8Fe and 7Fe forms in order to distinguish between signals that arise from the convertible [4Fe-4S] cluster and those produced by the non-convertible [4Fe-4S] cluster. In both these proteins, the 8Fe forms show oxidation peaks that are not present in the 7Fe voltammetry; these are at +420 mV (native) and +532 mV ($\Delta\text{Thr}^{14}/\Delta\text{Asp}^{15}$), and must derive from the [4Fe-4S] cluster that is only present in the 8Fe protein. Also observed at higher potentials are oxidation peaks that are similar in both the 8Fe and 7Fe forms of these proteins; these are therefore produced by the [4Fe-4S] cluster present in both forms of these proteins.

High-potential voltammetry of the 8Fe form of T14C *AvFdI* reveals a larger peak at +610 mV that is not observed in the 7Fe form. The latter displays two overlapping signals at a higher potential than in the 8Fe form, with the lower potential peak appearing at +670 mV.

With C42D *AvFdI*, for which the single [4Fe-4S] cluster can be oxidized to give a second [3Fe-4S] cluster, a comparison between 7Fe and 6Fe forms is required. Importantly, the 7Fe form of this protein displays a high-potential oxidative peak at +672 mV, whereas the 6Fe form, which does not contain any [4Fe-4S] clusters, exhibits no peaks in this high-potential region.

High-potential voltammetry of *DaFdIII*, *TaFd* and *PfFd*

To investigate cluster degradation further, three other ferredoxins, which contain either a [4Fe-4S] cluster *in vivo* (*PfFd* and *TaFd*) or a [3Fe-4S] cluster that can be converted into a [4Fe-4S] cluster *in vitro* (*DaFdIII*), were examined. Figure 9 shows the oxidative peaks seen from high-potential voltammetry for different forms of these proteins, along with *AvFdI* for comparison. As with *AvFdI* and its variants, no corresponding high-potential reduction peaks were observed on the subsequent sweep in the negative direction.

DaFdIII is a 7Fe protein *in vivo* which readily takes up Fe^{2+} from solution to form an 8Fe protein *in vitro* [5,6,20]. The [4Fe-4S] $^{2+/+}$ cluster formed is extremely labile, and if no Fe^{2+} is present in solution it returns to the [3Fe-4S] form, even when electrochemically poised to 'lock' it in the 2+ oxidation level. In any event, complete conversion is achieved after a 60 s pulse at +200 mV [5]. Figure 9 shows the high-potential voltammetry of the 7Fe and 8Fe forms of *DaFdIII*. Both the 7Fe form (in 2 mM EGTA) and the 8Fe form reveal a large peak at +726 mV, while the 8Fe form exhibits an extra peak at +434 mV.

The ferredoxin (*TaFd*) from the denitrifying bacterium *T. aromatica* contains two [4Fe-4S] clusters [30]. Figure 9 shows that the high-potential voltammetry of *TaFd* displays a large asymmetric peak at +609 mV. When pulsed in normal buffer solution or in the presence of 2 mM EGTA, a large degree of

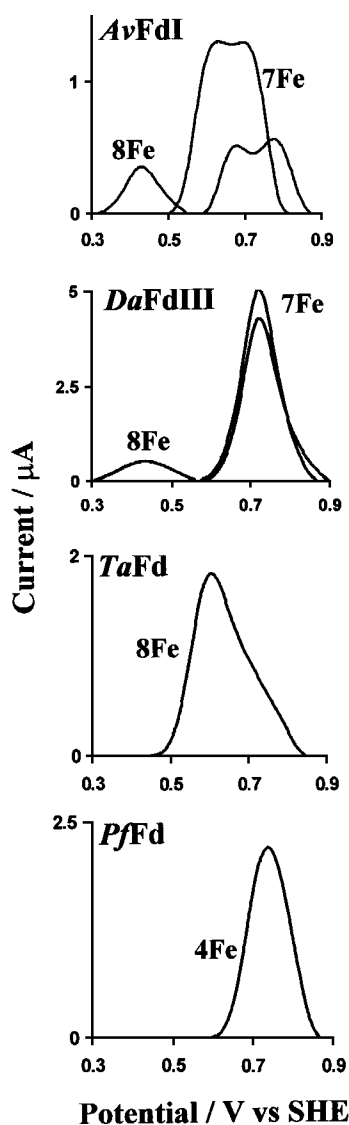


Figure 9 High-potential voltammograms (background-subtracted, oxidation direction only) recorded for *AvFdl*, *DaFdlIII*, *TaFd*, *CpFd* and *PfFd*

All voltammograms were recorded at pH 7.0, 0 °C. SHE, standard hydrogen electrode.

signal loss was evident. Pulses (4 s duration) at potentials above +568 mV resulted in almost total signal loss, and there was no evidence for formation of [3Fe-4S] clusters.

The hyperthermophile *P. furiosus*, which grows optimally at 100 °C, produces a ferredoxin (*PfFd*) that contains one [4Fe-4S] cluster, one Fe atom of which is co-ordinated by aspartate (Figure 1) [28,39]. Incubation with excess ferricyanide converts this cluster into the [3Fe-4S] form [38]. Both forms were subjected to high-potential voltammetry: for the [4Fe-4S] form, a symmetrical oxidative peak was observed at +744 mV (Figure 9), whereas the [3Fe-4S] form gave no signal, similar to the all-[3Fe-4S] (6Fe) form of C42D *AvFdl*.

Irreversibility and size of high-potential peaks

In the high-potential voltammetry of all the proteins studied, no corresponding reductive peaks were observed. This irreversibility

was investigated using fast-scan voltammetry, for which CVs recorded at scan rates as fast as $8 \text{ V} \cdot \text{s}^{-1}$ failed to reveal any reduction peaks to accompany oxidation. Consequently, the peaks relate only approximately to true reduction potentials of processes. Scanning in the low-potential region immediately after a fast-scan CV past the higher-potential peak revealed that all protein film signals had vanished.

The number of electrons involved in the oxidative processes was estimated by comparing the areas with the one-electron signals for the normal [4Fe-4S]^{2+/+} and [3Fe-4S]^{+/0} couples. For all proteins, this procedure gave values of 10 ± 3 electrons for the process at highest potential: however, in 8Fe forms of native *AvFdl*, $\Delta\text{Thr}^{14}/\Delta\text{Asp}^{15}$ *AvFdl* and *DaFdlIII*, the areas of the clearly separated peaks at more negative potential (420 mV, +532 mV and 434 mV respectively) are much smaller, at approx. two electrons. The peak at +420 mV seen for the 8Fe form of *AvFdl* was investigated by fast-scan voltammetry. When swept to +693 mV at $100 \text{ V} \cdot \text{s}^{-1}$, cluster conversion failed to occur, although sweeping at $50 \text{ V} \cdot \text{s}^{-1}$ produced conversion into the 7Fe form, as expected. Despite these high rates, no corresponding reduction peak was observed, showing that cluster degradation induced by oxidation is very fast.

DISCUSSION

Pulsed oxidation of [4Fe-4S] clusters and the formation of [3Fe-4S] products

The results we have described show how oxidative pulses applied to proteins containing [4Fe-4S] clusters induce degradation, and in many cases [3Fe-4S] clusters are observed as products. In *CpFd* the stability of the [4Fe-4S] clusters and their conversion into [3Fe-4S] forms were found to relate to irreversible signals observed at high potentials [13]. CV and pulsing reveal this also to be the case with the proteins examined in this study, where in most cases the potentials of the oxidation peaks correlate with the conversion of [4Fe-4S] into [3Fe-4S] clusters.

The high-potential voltammograms vary in complexity. Significantly, those proteins containing only [3Fe-4S] clusters gave little detectable signal, those with one [4Fe-4S] cluster gave one signal, while those containing two [4Fe-4S] clusters gave rise to two signals. The signals thus associated with [4Fe-4S] clusters often showed more than one component, but these could not be resolved or interpreted. In no case were reduction peaks detected on the return sweep of CVs scanned between 0 and 900 mV. It is not clear if this irreversibility arises from protein desorption or very rapid degradation of the oxidized Fe-S species.

The larger peaks involve multiple-electron reactions, up to approx. 10 electrons (referenced to the low-potential one-electron couples), so it is certain that much of the signal loss stems from destruction of the [4Fe-4S] cluster and oxidation of its components, i.e. the Fe^{2+} and S^{2-} ions. As an example, voltammetry that engaged the large oxidative peak produced by 7Fe C42D *AvFdl* was irreversible even at scan rates as fast as $8 \text{ V} \cdot \text{s}^{-1}$, and scanning the normal region immediately after an excursion above the higher potential oxidative peak revealed that all film signals had disappeared; therefore the processes responsible for complete cluster degradation and/or film loss are rapid.

Significantly, the 8Fe forms of native *AvFdl*, $\Delta\text{Thr}^{14}/\Delta\text{Asp}^{15}$ *AvFdl* and *DaFdlIII* clearly display relatively small oxidation peaks at less positive potentials, i.e. +420 mV, +532 mV and +434 mV respectively, which are not present in respective 7Fe forms. The areas of these peaks are approximately as expected for a two-electron reaction, and the voltammograms that are subsequently recorded in the normal potential region reveal that a [3Fe-4S] cluster has been formed. The stoichiometry

Table 1 Reduction potentials of interconverting [4Fe-4S] and [3Fe-4S] clusters

Reduction potentials shown are in mV as measured against the standard hydrogen electrode. Native and T14C *AvFdI* values refer to pH 7.4; the $\Delta\text{Thr}^{14}/\Delta\text{Asp}^{15}$ and C42D mutants refer to pH 7.0.

Mutant	Fe-S cluster ...	Reduction potential				
		[3Fe-4S] ^{+ / 0}	New [3Fe-4S] ^{+ / 0}	[4Fe-4S] ^{2+ / +}	New [4Fe-4S] ^{2+ / +}	[3Fe-4S] ^{0 / 2-}
7Fe native		-420		-641		-0.756
8Fe native				-615	-551	
7Fe $\Delta\text{Thr}^{14}/\Delta\text{Asp}^{15}$		-147		-636		-0.748
8Fe $\Delta\text{Thr}^{14}/\Delta\text{Asp}^{15}$				-642	-466	
7Fe T14C		-426		-633		-0.756
8Fe T14C				-565	-519	
7Fe C42D		-398		-643		Not measured
6Fe C42D			-297			

suggests that these peaks are produced by oxidation of [4Fe-4S]²⁺ to the 3+ state and immediate oxidation of released Fe²⁺, without catastrophic breakdown.

Oxidative pulse experiments relate the amount of [3Fe-4S] cluster formed to the potential applied during the pulse. For 8Fe $\Delta\text{Thr}^{14}/\Delta\text{Asp}^{15}$ *AvFdI*, a rough analysis fitting of the data to a Nernstian sigmoid gives a reduction potential of +540 mV for the process of cluster conversion. The value is similar to that of the oxidation peak at +532 mV, supporting the idea that it is this peak, which is not observed in the 7Fe form, that must be accessed to induce cluster conversion. For C42D *AvFdI*, an oxidative peak at +672 mV is observed only in the 7Fe form, showing that this process is due to the [4Fe-4S] cluster. As with $\Delta\text{Thr}^{14}/\Delta\text{Asp}^{15}$ *AvFdI*, this value agrees with an estimate of +670 mV that is obtained on the basis of a Nernstian fit to the data for [3Fe-4S] formation.

Formation of [3Fe-4S]^{+ / 0} clusters at the electrode surface was not observed in T14C *AvFdI*, *TaFd* or *PfFd*. Subjecting films to pulses or excursions to varying oxidizing potentials produced no new signals due to [3Fe-4S] clusters, only an attenuation of the signals due to [4Fe-4S]^{2+ / +} which could be the result of cluster degradation or protein desorption. The result for *PfFd* appears at first somewhat surprising, since formation of [3Fe-4S] can be induced by excess [Fe(CN)₆]³⁻; however, the [4Fe-4S] form is quite stable to air [38].

Changes in redox properties due to [4Fe-4S]/[3Fe-4S] interconversions

Iron-sulphur clusters are widely used in biology as electron-transfer agents, and interconversion between [4Fe-4S] and [3Fe-4S] forms provides a relatively easy mechanism for varying reduction potential in the same protein, a feature that might be important for physiological function. Table 1 shows the potentials of the interconverting clusters examined in this study.

In agreement with results for other interconverting 3Fe/4Fe systems, the [3Fe-4S]^{+ / 0} clusters have potentials between 93 and 350 mV, more positive than those of their [4Fe-4S]^{2+ / +} counterparts. While reduction potentials for the + / 0 couple vary by over 250 mV for different [3Fe-4S] clusters, those for the 0 / 2- couple, which is always linked to protonation that compensates electrostatically for the electron transfers, vary only by about 100 mV [21]. The observation that the all-[3Fe-4S] forms of C42D *AvFdI* and *PfFd* exhibit no peaks in the high-potential region is consistent with the results for *CpFd*, which showed that

the [3Fe-4S] clusters produced by oxidation of [4Fe-4S] clusters are relatively resistant to further oxidative damage [13].

Correlation between the potentials for electrochemical oxidation of [4Fe-4S] clusters and air sensitivity

We can now attempt to correlate the oxidation peak potentials associated with [4Fe-4S] clusters with their air-sensitivities. Quantitative data on air-sensitivities of different iron-sulphur proteins are not available, but observations have been made on the proteins we have studied, and reactivities with other oxidants such as Fe(CN)₆³⁻ have been reported.

First, considering the variants of *AvFdI*: each form has a different sensitivity to air, ranging from 8Fe reconstituted native *AvFdI*, which is extremely air-sensitive, to C42D, which resists degradation by common chemical oxidants, with $\Delta\text{Thr}^{14}/\Delta\text{Asp}^{15}$ and T14C *AvFdI* lying between these extremes. Figure 10 shows the relationships between cluster stability on exposure to oxygen and the potential of the [4Fe-4S] oxidation process (the 'transition potential') that coincides with the formation of [3Fe-4S], and may tentatively be identified with the [4Fe-4S]^{3+ / 2+} redox couple.

The air-sensitive 8Fe forms of native and $\Delta\text{Thr}^{14}/\Delta\text{Asp}^{15}$ *AvFdI* each show small oxidation peaks (+420 mV and +532 mV respectively) at lower potential than the more stable variants, and a [3Fe-4S] cluster is detected after accessing this region. The 8Fe form of T14C *AvFdI* and the 7Fe form of C42D *AvFdI* are less air-sensitive: they display larger oxidation peaks at higher potentials (+610 mV and +672 mV respectively) suggestive of more catastrophic degradation, and indeed only in the case of C42D could a [3Fe-4S] cluster be detected in the oxidation product. The air-stable [4Fe-4S] cluster in C42D *AvFdI* resists chemical oxidation, and has only been converted into a [3Fe-4S] cluster with the electrochemical pulsing method used in this paper [26].

DaFdIII is isolated as a 7Fe protein, which takes up Fe²⁺ in solution to form a very labile 8Fe protein; therefore the stability of the [4Fe-4S] cluster created *in vitro* was anticipated to be similar to that of the highly unstable cluster in 8Fe *AvFdI*, which produces a peak at +420 mV. As expected, 8Fe *DaFdIII* gives a peak at +434 mV that is not present in the 7Fe form. *PfFd* contains a [4Fe-4S] cluster *in vivo* and this is only slowly converted into the [3Fe-4S] form in air [38,40]. Accordingly, our results show that electrochemically it is also quite inert and the large peak that is observed at +744 mV does not relate to formation of [3Fe-4S] clusters. *TaFd* is not known to be air-sensitive and,

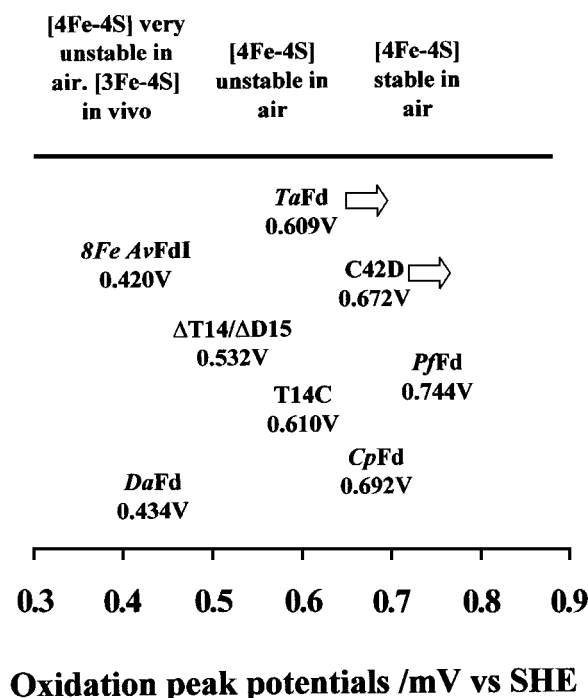


Figure 10 Correlations between air-sensitivities of AvFdl variants and other ferredoxins, and their oxidative transformation potentials measured by voltammetry

Arrows indicate where the observed sensitivity to air does not correlate well with the oxidative transformation potential. SHE, standard hydrogen electrode.

as expected, no [3Fe-4S] cluster is detected after oxidative pulses or excursions through the large peak at +609 mV. CpFd is mildly air-sensitive; EPR signals due to [3Fe-4S]⁺ become observable upon extended contact with air, or after treatment with Fe(CN)₆³⁻ [29]. In pulsing experiments, both [4Fe-4S] clusters could be converted into [3Fe-4S] and the high-potential voltammetry showed a peak at +692 mV [13].

In conclusion, within the group of AvFdl variants, there is a fairly good correlation between air-sensitivity, facile formation of (or isolation as) a [3Fe-4S] cluster, and the appearance of a limited oxidation process at relatively low potential (< +450 mV). Oxidation processes at higher potential appear also to produce more extensive (and irreversible) cluster degradation. Further generalizations predicting the air-sensitivities of other proteins have limited success. The extreme sensitivity of DaFdIII is not surprising, given that Fe is released readily even without oxidation, while 8Fe TaFd appears more air-stable than 8Fe CpFdIII, despite showing oxidation processes at lower potential (+609 compared with +692 mV: for reference, C42D with a value of +672 mV is also air-stable). It seems that the potentials of oxidation processes are an approximate, but not absolute, guide to [4Fe-4S] cluster sensitivity.

In HiPIPs, the [4Fe-4S]^{3+/2+} cluster is buried within the protein in a hydrophobic pocket. Mutants of *Allochromatium vinosum* HiPIP in which solvent accessibility has been increased show relatively little variation in the [4Fe-4S]^{3+/2+} reduction potential, but exhibit marked instability towards oxidative degradation [14–17]. Therefore, in these proteins, conversion of [4Fe-4S]³⁺ into [3Fe-4S] (or total degradation) is prevented by shielding the cluster from water. In contrast, for most proteins that contain

[4Fe-4S]^{2+/+} clusters, the key factor in determining stability with respect to oxygen and oxidizing conditions may be the thermodynamic ease of oxidation to the 3+ level.

We thank Dr. M. Boll and Dr. E.C. Hatchikian for the samples of TaFd and DaFdIII. This research was supported by grants from BBSRC 43/B11675 (F.A.A.), EPSRC GR/J84809 (G.J.T. and F.A.A.), National Institute of Health Grants GM-45209 (B.K.B.) and The National Council of Science and Technology of Mexico (CONACYT) (R.C.).

REFERENCES

- Beinert, H., Holm, R. H. and Münck, E. (1997) Iron–sulfur clusters: Nature's modular, multipurpose structures. *Science* **277**, 653–659
- Beinert, H., Kennedy, M. C. and Stout, C. D. (1996) Aconitase as iron–sulfur protein, enzyme and iron-regulatory protein. *Chem. Rev.* **96**, 2335–2373
- Beinert, H. (2000) Iron-sulfur proteins: ancient structures, still full of surprises. *J. Biol. Inorg. Chem.* **5**, 2–15
- Fawcett, S. E. J., Davis, D., Breton, J., Thomson, A. J. and Armstrong, F. A. (1998) Voltammetric studies of the reactions of iron-sulphur clusters ([3Fe-4S] or [M3Fe-4S]) formed in *Pyrococcus furiosus* ferredoxin. *Biochem. J.* **335**, 357–368
- Butt, J. N., Fawcett, S. E. J., Breton, J., Thomson, A. J. and Armstrong, F. A. (1997) Electrochemical potential and pH dependences of [3Fe-4S] ↔ [M3Fe-4S] cluster transformations (M = Fe, Zn, Co and Cd) in ferredoxin III from *Desulfovibrio africanus* and detection of a cluster with M = Pb. *J. Am. Chem. Soc.* **119**, 9729–9737
- George, S. J., Armstrong, F. A., Hatchikian, E. C. and Thomson, A. J. (1989) Electrochemical and spectroscopic characterization of the conversion of the 7Fe into the 8Fe form of Ferredoxin-III From *Desulfovibrio africanus*—Identification of a [4Fe-4S] Cluster with one non-cysteine ligand. *Biochem. J.* **264**, 275–284
- Beinert, H. and Albracht, S. P. J. (1982) New insights, ideas and unanswered questions concerning iron-sulfur clusters in mitochondria. *Biochim. Biophys. Acta* **683**, 245–277
- Johnson, M. K., Morningstar, J. E., Cecchini, G. and Ackrell, B. A. C. (1985) *In vivo* detection of a 3 iron cluster in fumarate reductase from *Escherichia coli*. *Biochem. Biophys. Res. Commun.* **131**, 653–658
- Johnson, M. K., Morningstar, J. E., Ackrell, B. A. C., Kearney, E. B. and Maguire, J. J. (1985) Evidence for [2Fe-2S], [3Fe-XS], and [4Fe-4S] clusters in succinate dehydrogenase. *Fed. Proc.* **44**, 675
- Johnson, M. K., Morningstar, J. E., Bennett, D. E., Ackrell, B. A. C. and Kearney, E. B. (1985) Magnetic circular dichroism studies of succinate dehydrogenase—evidence for [2Fe-2S], [3Fe-XS], and [4Fe-4S] centers in reconstitutively active enzyme. *J. Biol. Chem.* **260**, 7368–7378
- Morningstar, J. E., Johnson, M. K., Cecchini, G., Ackrell, B. A. C. and Kearney, E. B. (1985) The high-potential iron-sulfur center in *Escherichia coli* fumarate reductase is a three-iron cluster. *J. Biol. Chem.* **260**, 3631–3638
- Teixeira, M., Moura, I., Xavier, A. V., Dervartanian, D. V., LeGall, J., Huynh, B. H. and Moura, J. J. G. (1983) *Desulfovibrio gigas* hydrogenase—redox properties of the nickel and iron-sulfur centers. *Eur. J. Biochem.* **130**, 481–484
- Camba, R. and Armstrong, F. A. (2000) Investigations of the oxidative disassembly of Fe-S clusters in *Clostridium pasteurianum* ferredoxin using pulsed protein film voltammetry. *Biochemistry* **34**, 10587–10598
- Soriano, A. and Cowan, J. A. (1996) Phenylalanine 48 of *Chromatium vinosum* high potential iron protein is essential for stability of the oxidized [Fe₄S₄] cluster. Site-directed mutagenesis and NMR studies as a probe of cluster chemistry. *Inorg. Chim. Acta* **251**, 285–290
- Soriano, A., Li, D. W., Bian, S. M., Agarwal, A. and Cowan, J. A. (1996) Factors influencing redox thermodynamics and electron self-exchange for the [Fe₄S₄] cluster in *Chromatium vinosum* high potential iron protein: the role of core aromatic residues in defining cluster redox chemistry. *Biochemistry* **35**, 12479–12486
- Bian, S. M., Hemann, C. F., Hille, R. and Cowan, J. A. (1996) Characterization of an auto-reduction pathway for the [Fe₄S₄]³⁺ cluster of mutant *Chromatium vinosum* high-potential iron proteins—site-directed mutagenesis studies to probe the role of phenylalanine 66 in defining the stability of the [Fe₄S₄] center provide evidence for oxidative degradation via a [Fe₃S₄] cluster. *Biochemistry* **35**, 14544–14552
- Cowan, J. A. and Lui, S. M. (1998) Structure–function correlations in high-potential iron proteins. *Adv. Inorg. Chem.* **45**, 313–350
- Armstrong, F. A. (1997) Applications of voltammetric methods for probing the chemistry of redox proteins. *Bioelectrochemistry of Biomacromolecules*, vol. 5 (Lenaz, G. and Milazzo, G., eds.), pp. 205–235, Birkhauser, Basel
- Armstrong, F. A., Heering, H. A. and Hirst, J. (1997) Reactions of complex metalloproteins studied by protein-film voltammetry. *Chem. Soc. Rev.* **26**, 169–179

- 20 Butt, J. N., Armstrong, F. A., Breton, J., George, S. J., Thomson, A. J. and Hatchikian, E. C. (1991) Investigation of metal-ion uptake reactivities of [3Fe-4S] clusters in proteins—voltammetry of co-adsorbed ferredoxin aminocyclitol films at graphite electrodes and spectroscopic identification of transformed clusters. *J. Am. Chem. Soc.* **113**, 6663–6670
- 21 Duff, J. L. C., Breton, J. L. J., Butt, J. N., Armstrong, F. A. and Thomson, A. J. (1996) Novel redox chemistry of [3Fe-4S] clusters: Electrochemical characterization of the all-Fe(II) form of the [3Fe-4S] cluster generated reversibly in various proteins and its spectroscopic investigation in *Sulfolobus acidocaldarius* ferredoxin. *J. Am. Chem. Soc.* **118**, 8593–8603
- 22 Hirst, J., Jameson, G. N. L., Allen, J. W. A. and Armstrong, F. A. (1998) Very rapid, cooperative two-electron/two-proton redox reactions of [3Fe-4S] clusters: detection and analysis by protein-film voltammetry. *J. Am. Chem. Soc.* **120**, 11994–11999
- 23 Morgan, T. V., Stephens, P. J., Burgess, B. K. and Stout, C. D. (1984) Reconstitution of *Azotobacter vinelandii* ferredoxin I as a 2[4Fe-4S]^{2+/+} protein. *FEBS Lett.* **167**, 137–141
- 24 Kemper, M. A., Gao-Sheridan, H. S., Shen, B. H., Duff, J. L. C., Tilley, G. J., Armstrong, F. A. and Burgess, B. K. (1998) $\Delta T14/\Delta D15$ *Azotobacter vinelandii* ferredoxin I: Creation of a new CysXXCysXXCys motif that ligates a [4Fe-4S] cluster. *Biochemistry* **37**, 12829–12837
- 25 Gao-Sheridan, H. S., Kemper, M. A., Khayat, R., Tilley, G. J., Armstrong, F. A., Sridhar, V., Prasad, G. S., Stout, C. D. and Burgess, B. K. (1998) A T14C variant of *Azotobacter vinelandii* ferredoxin I undergoes facile [3Fe-4S]⁰ to [4Fe-4S]²⁺ conversion *in vitro* but not *in vivo*. *J. Biol. Chem.* **273**, 33692–33701
- 26 Jung, Y.-S., Bonagura, C. A., Tilley, G. J., Gao-Sheridan, H. S., Armstrong, F. A., Stout, C. D. and Burgess, B. K. (2000) Structure of C42D *Azotobacter vinelandii* ferredoxin I: a CysXXAspXXXys motif ligates an air-stable [4Fe-4S]^{2+/+} cluster. *J. Biol. Chem.* **275**, 36974–36983
- 27 Armstrong, F. A., George, S. J., Cammack, R., Hatchikian, E. C. and Thomson, A. J. (1989) Electrochemical and spectroscopic characterization of the 7Fe Form of ferredoxin III From *Desulfovibrio africanus*. *Biochem. J.* **264**, 265–273
- 28 Aono, S., Bryant, F. O. and Adams, M. W. W. (1989) A novel and remarkably thermostable ferredoxin from the hyperthermophilic archaeobacterium *Pyrococcus furiosus*. *J. Bacteriol.* **171**, 3433–3439
- 29 Thomson, A. J., Robinson, A. E., Johnson, M. K., Cammack, R., Rao, K. K. and Hall, D. O. (1981) Low-temperature magnetic circular dichroism evidence for the conversion of 4-iron-sulfur clusters in a ferredoxin from *Clostridium pasteurianum* into 3-iron-sulfur clusters. *Biochim. Biophys. Acta* **637**, 423–432
- 30 Boll, M., Fuchs, G., Tilley, G. J., Armstrong, F. A. and Lowe, D. (2000) Unusual spectroscopic and electrochemical properties of the 2[4Fe-4S] ferredoxin of *Thaueria aromatica*. *Biochemistry* **39**, 4929–4938
- 31 Shen, B. H., Martin, L. L., Butt, J. N., Armstrong, F. A., Stout, C. D., Jensen, G. M., Stephens, P. J., Lamar, G. N., Gorst, C. M. and Burgess, B. K. (1993) *Azotobacter vinelandii* ferredoxin-I-Aspartate-15 facilitates proton transfer to the reduced [3Fe-4S] cluster. *J. Biol. Chem.* **268**, 25928–25939
- 32 Armstrong, F. A., Butt, J. N. and Sucheta, A. (1993) Voltammetric studies of redox-active centers in metalloproteins adsorbed on electrodes. *Methods Enzymol.* **227**, 479–500
- 33 Herring, H. A., Weiner, J. H. and Armstrong, F. A. (1997) Direct detection and measurement of electron relays in a multicentered enzyme: voltammetry of electrode-surface films of *E. coli* fumarate reductase, an iron-sulfur flavoprotein. *J. Am. Chem. Soc.* **119**, 11628–11638
- 34 Stephens, P. J., Morgan, T. V., Devlin, F., Penner-hahn, J. E., Hodgson, K. O., Scott, R. A., Stout, C. D. and Burgess, B. K. (1985) [4Fe-4S] cluster-depleted *Azotobacter vinelandii* ferredoxin-I: a new 3Fe iron-sulfur protein. *Proc. Natl. Acad. Sci. U.S.A.* **82**, 5661–5665
- 35 Finnegan, M. G., Conover, R. C., Park, J. B., Zhou, Z. H., Adams, M. W. W. and Johnson, M. K. (1995) Electronic, magnetic, redox and ligand-binding properties of [MFe₃S₄] clusters (M = Zn, Co, Mn) in *Pyrococcus furiosus* ferredoxin. *Inorg. Chem.* **34**, 5358–5369
- 36 Moura, I., Moura, J. J. G., Münck, E., Papaefthymiou, V. and LeGall, J. (1986) Evidence for the formation of a [CoFe₃S₄] cluster in *Desulfovibrio gigas* ferredoxin II. *J. Am. Chem. Soc.* **108**, 349–351
- 37 Chen, K., Hirst, J., Camba, R., Bonagura, C. A., Stout, C. D., Burgess, B. K. and Armstrong, F. A. (2000) Atomically defined mechanism for electron-coupled proton transfer to a buried redox centre in a protein. *Nature (London)* **405**, 814–817
- 38 Conover, R. C., Kowal, A. T., Fu, W., Park, J. B., Aono, S., Adams, M. W. W. and Johnson, M. K. (1991) Spectroscopic characterization of the novel iron-sulfur cluster in *Pyrococcus furiosus* ferredoxin. *J. Biol. Chem.* **265**, 8533–8541
- 39 Calzolari, L., Gorst, C. M., Zhao, Z.-H., Teng, Q., Adams, M. W. W. and La Mar, G. N. (1995) ¹H-NMR investigation of the electronic and molecular structure of the 4Fe cluster ferredoxin from the hyperthermophile *Pyrococcus furiosus*—Identification of asp-14 as a cluster ligand in each of the four redox states. *Biochemistry* **34**, 11373–11384
- 40 Brereton, P. S., Verhagen, M. F., Zhou, Z. H. and Adams, M. W. W. (1998) Effect of iron-sulfur cluster environment in modulating the thermodynamic properties and biological function of ferredoxin from *Pyrococcus furiosus*. *Biochemistry* **37**, 7351–7362

Received 25 July 2001/3 October 2001; accepted 8 October 2001